Mean-field simulation of hopping resistivity in a model with Coulomb interactions and current correlations

A. Avdonin*

Institute of Physics, Polish Academy of Sciences, Al. Lotników 32/46, 02-668 Warszawa, Poland

Physica B 608 (2021) 412871

Abstract

Simulations of hopping resistivity by mean-field methods rely on randomly generated site energies. Thus such effects as the presence of the Coulomb gap and electron current correlations have been simulated using predominantly Monte Carlo methods. This paper presents a method of mean-field calculation of hopping resistivity in a wide range of temperatures and electric fields. This method considers the long-range Coulomb interactions and at least partially accounts for the electron current correlations. Resulting curves reproduce the Mott law in the form predicted by Efros and Shklovskii and the experimentally observed electric field dependencies. Based on the results, a decrease of hopping energy is predicted with increasing temperature in the nearest-neighbor hopping regime. The report analyses the differences between the mean-field and the Monte Carlo approaches.

1. Introduction

The simulation of electron transport in the hopping regime remains a challenging task. In this regime, charge carriers propagate in a solid by phonon-assisted tunneling through a random network of localized sites. Such propagation is probabilistic in the sense that carriers can, in principle, jump to any of the surrounding sites. The probability of each jump depends exponentially on the distance between sites and on the energy barrier between them. The analysis of all possible propagation paths in the presence of broad distributions of jump distances and jump barriers is a formidable task itself, even for relatively small cells.

The problem is also difficult because the carriers interact with each other and with ions via strong, long-range Coulomb interactions. Because of this, the energies of a large number of states change significantly after each jump. This requires frequent recalculation of site energies during the simulation.

Another complication is that each site can hold only a single electron (if the upper Hubbard band is not considered). This imposes additional restrictions on the possible jumps and results in correlations (called Hubbard current correlations) in the positions of individual carriers, which ought to be taken into account.

Because of the complexity of the problem there is a variety of approaches to the simulation of hopping conductivity, which differ by calculation methods and by amount of approximations employed. The most popular simulation methods of hopping conductance are Monte Carlo (MC) simulation and solution of balance equations (BE) methods. The latter is usually referred to as the master equation method. Each method has its advantages and disadvantages.

The MC simulation methods are the closest to simulating all of the above phenomena. In this sense, they are considered to be the most exact and are often used to test theories and other models. One disadvantage of MC methods is due to the "soft" pairs and clusters, which attract the attention of the algorithm without producing a net current. Although there are methods of restricting the soft pairs, the MC calculations become less practical at low electric fields and at low temperatures. Another disadvantage is that the dependencies obtained using the MC methods are noisy. This is the effect of the random nature of simulated jumps which, (i) modify the occupation of sites by discrete amounts and (ii) result in a random set of paths explored in each simulation.

The BE method is a mean-field method. In this method some averaged values of occupation are attributed to all impurity sites. The transport is calculated assuming these averaged values of occupations. The BE method considers all possible current paths simultaneously. It allows for continuous variation of occupation and produces smooth curves. It is based on the solution of sets of equations and can be used at low temperatures and low electric field conditions. However, it requires the appropriately averaged energies of all sites to be provided by some other method. In all known to me reports, regarding the resistivity calculation using mean-field approach, some random energies uncorrelated with the site positions were assigned to localized sites. Because the averaged equilibrium values of occupation are used in mean-field methods, the accounting for the Hubbard current correlations in the mean-field approach is an active area of research. If the mentioned correlations are disregarded the results obtained using the BE approach are in agreement with the results of MC simulations and are produced in less time.

*Corresponding author
Email address: avdonin@ifpan.edu.pl (A. Avdonin)

The goal of this work was to simulate differentiable temperature dependencies of resistivity in hopping regime in a wide temperature range. For this reason, the mean-field approach to simulations was chosen. The goal was also to use as few simplifications as possible. The presented algorithm accounts for the long-range Coulomb interaction in the system. It simulates the Coulomb gap in the density of states at low temperatures and the filling of the Coulomb gap at higher temperatures. It takes into account the energy-distance correlations for electron transitions and partially accounts for the Hubbard current correlations. The simulations were carried out for a 3D system of point defects randomly distributed in a cell.

Section 2 shows how the site energies and equilibrium occupations were calculated for the balance equation method. Section 3 shows how hopping resistivity was calculated. Section 4 shows how the system of balance equations was solved. Section 5 summarizes the entire calculation procedure. Section 6 shows samples of calculated dependencies. The final section is devoted to discussion.

2. Mean-field occupation and site energies

Let us consider a three-dimensional system of N_d donor point defects randomly distributed inside a cube-shaped cell of size L. Inside the cell there are also randomly distributed N_a compensating acceptor defects $N_a = bN_d$, where b is the coefficient of compensation. The Hamiltonian of the system is

$$H = \frac{e^2}{\kappa}\left[\frac{1}{2}\sum_{m\neq n}\frac{1}{R^a_{mn}} - \sum_{i,m}\frac{1-n_i}{R_{im}} + \frac{1}{2}\sum_{i\neq j}\frac{(1-n_i)(1-n_j)}{r_{ij}}\right]. \quad (1)$$

Here, e is the electron charge, $k = 1/4\pi\epsilon\epsilon_0$. The first term represents Coulomb interaction between ionized acceptors, the second term represents interaction between ionized donors and acceptors and the last term represents the interaction between ionized donors. R^a_{mn}, $R_{i,m}$, $r_{i,j}$ stand for acceptor-acceptor, acceptor-donor and donor-donor distances, respectively. Variable n_i is the occupation of donor site i. In the mean-field approximation it can have any value in the range $[0, 1]$. The purpose of this section is to calculate the distribution of n_i at any temperature.

In the following text, length is measured in the units of average donor-donor distance d_0 and energy in the units of $\varepsilon_0 = e^2/\kappa d_0$. It is suitable to set the origin of the energy axis to

$$H_0 = \frac{1}{2}\sum_{m\neq n}\frac{1}{R^a_{mn}} - \sum_{i,m}\frac{1}{R_{im}} + \frac{1}{2}\sum_{i\neq j}\frac{1}{r_{ij}} = 0 \quad (2)$$

Here H_0 is the energy of Coulomb interaction of all nuclei of the system. Then the Hamiltonian is reduced to

$$H = \sum_i n_i\left[\varphi_i + \frac{1}{2}\sum_{j\neq i}\frac{n_j}{r_{ij}}\right], \quad (3)$$

and contains only the electron-related parts. Here the second term represents electron-electron interaction, and φ_i is the energy of the i-th electron in the field of all nuclei, which depends on system geometry only.

$$\varphi_i = \sum_{j\neq i}\frac{1}{R_{ij}} - \sum_{j\neq i}\frac{1}{r_{ij}}. \quad (4)$$

Values of n_i are usually calculated using a Monte Carlo approach. However, it was demonstrated analytically that if one assigns each site a parameter ε_i, which is measured in units of energy,

$$\varepsilon_i \equiv \varphi_i + \sum_{j\neq i}\frac{n_j}{r_{ij}}, \quad (5)$$

then n_i follows the Fermi-Dirac statistics with respect to ε_i

$$n_i = \frac{1}{1+\exp(\beta(\varepsilon_i-\mu))}. \quad (6)$$

Here $\beta = 1/k_BT$, T is temperature, k_B is Boltzmann constant, and μ is Fermi energy. It is a surprising result, since electrons in the considered system are strongly interacting, no quasi-particles were introduced, and $H \neq \sum n_i\varepsilon_i$. Energy ε_i has the meaning of energy released by adding an external electron into an empty state i or energy required to remove an electron from an occupied state i to the infinity, i.e. energy of transfer of an electron from and to the vacuum level. This result was verified by Monte Carlo simulations for a 2D system in a limited range of temperatures.

This result makes it possible to calculate n_i and ε_i relatively easy using numerical methods. Substitution of Eq. (6) into Eq. (5) gives a system of equations which can be solved with respect to ε_i

$$\varepsilon_i = \varphi_i + \sum_{j\neq i}\frac{1}{r_{ij}[1+\exp(\beta(\varepsilon_j-\mu))]}, \quad (7)$$

and then the occupation of the sites can be calculated from Eq. (6). To solve this system of equations, the Fermi energy μ needs to be calculated using the charge neutrality condition $\sum n_i = N_d(1-b)$ or

$$\sum\frac{1}{1+\exp(\beta(\varepsilon_i-\mu))} = N_d(1-b). \quad (8)$$

In this work the method of iterations was used to calculate ε_i, with iteration scheme given by Eq. (7). Values of ε_i were updated at once, such that the new values were used in all following calculations. The initial approximations of ε_i were calculated using Eq. (5) under the assumption that the electron charge is uniformly distributed among donors, $n_i = 1 - b$. Before each iteration, μ was calculated from Eq. (8) using bisection method. The search interval for μ was set between -10 and 10. Cyclic boundary conditions along x, y and z axes were assumed in the calculation of r_{ij} and R_{ij} using formula $r = \left(\Delta x^2 + \Delta y^2 + \Delta z^2\right)^{1/2}$, where

$$\Delta x = \min(|x_j - x_i|, L - |x_j - x_i|). \quad (9)$$

Values of Δy and Δz were calculated in a similar manner.

The described procedure robustly converges. The obtained site energies ε_i were used to calculate the energy distribution of

the DOS. Figure 1 shows such distributions for three temperatures $k_BT = 0.1$, 0.5 and 2. The compensation coefficient was set to $b = 0.5$. The distributions were obtained by combining noisy distributions of 100 randomly generated cells, each containing 500 donors. To combine the distributions of DOS of individual cells, they were shifted in energy to a common value of the Fermi energy, which was set to zero. For each realization of the cell, DOS was calculated as a histogram with 100 bars in the range from -5 to 5.

In the DOS calculated for $k_BT = 0.1$ the lower-energy band corresponds to occupied states $n_i \approx 1$, and the higher-energy band corresponds to empty states with $n_i \approx 0$. The dip in the DOS in the vicinity of the Fermi energy, called Coulomb gap, shows that energies ε_i calculated using mean-field approximation account for energy-position correlations which stem from the Coulomb interaction. The DOS at $k_BT = 0.1$ shown in Fig. 1 closely matches a similar dependence obtained by MC simulation for $T = 0$.

Gradual filling of the Coulomb gap occurs at higher temperatures as seen in Fig. 1. The Coulomb gap results from long-range Coulomb interaction and thus is observable only at low temperatures when the thermal energy is smaller than the Coulomb energy. When thermal energy is larger than the Coulomb energy, the distinction between occupied and unoccupied sites in the vicinity of the gap is gradually removed, as their occupation numbers tend to 0.5. Thus the distinct bands which appear at $T = 0$ in the DOS are expected to widen and to overlap at high temperatures.

This process was investigated in the literature using mean-field calculations and by MC method in a model 2D system and in a random 3D system with charged acceptors. Qualitatively there is an agreement in the evolution of the distribution of the DOS with temperature. However, the filling of the Coulomb gap occurs faster (at lower temperatures) in MC simulation than in mean-field simulations. This can also be seen if one compares present data from Fig. 1 and data from literature. This difference remains unexplained and has been attributed originally to the approximations of the mean-field approach.

One reason for such difference is that in MC approach relatively large amounts of charge (charge of one electron) are being moved at each jump. This produces large fluctuations in energy of all sites, and thus mixing of the bands of occupied and empty states occurs faster. In mean-field approach with the increasing temperature, the charge is continuously redistributed among sites, in fractions much smaller than electron charge. Thus, filling of the coulomb gap occurs slower and at a higher temperature.

There is also a discrepancy in the literature concerning the energy-distribution of the occupancy $n(\varepsilon)$ calculated using mean-field and MC approaches. The agreement is good again only at near-zero temperatures. The $n(\varepsilon)$ calculated using the MC method is steeper than the one calculated using mean-field approach.

My understanding is that $n(\varepsilon)$ calculated by mean-field and MC approaches should not be compared since they represent different quantities. In mean-field results, both n and ε are averaged values. In MC results, only n is averaged at equilibrium over time. The value of ε is not averaged and always represents the energy of the state at the moment of sampling. For this reason, in MC approach, a given site (say with index 1) will contribute to many bars of the distribution histogram since the energy of the site changes with time. On the other side, the same site will contribute to just one bar in the mean-field approach. Thus, in the distribution created using the MC approach the correlation between the occupation and the index (position in space) of the site is lost. Since hopping transport is sensitive to the relative positions of the sites, the result of MC approach seems to be less practical. This reasoning can be also applied to the earlier discussed discrepancy of DOS.

Because of how strong the site energy fluctuations are, the MC and mean-field approaches are not equivalent. In literature, the MC approach is used as the reference for other methods. However, the mean-field approach has some advantages, as shown in the following section and in the discussion.

3. Calculation of resistivity

The flow rate from a site i to another site j can be written as $\gamma_{ij}n_i(1-n_j)$. Here γ_{ij} is the quantum transition rate from the occupied site i to empty site j, n_i is probability of site i being occupied, and $1 - n_j$ is probability of site j being empty. The net flow of charge carriers between sites i and j is then

$$\gamma_{ij}n_i(1-n_j) - \gamma_{ji}n_j(1-n_i). \quad (10)$$

The electric current density of the entire cell can be calculated as

$$J = \frac{e\sum_{x=0}\left[\gamma_{ij}n_i(1-n_j) - \gamma_{ji}n_j(1-n_i)\right]}{L^2}. \quad (11)$$

Here the summation is made over pairs i, j, for which hopping occurs through some given cross-section of the cell (say at $x = 0$).

In this work, the intensity of the electric field is defined in terms of the average distance between donors d_0 and Coulomb energy ε_0 as follows

$$eEd_0 = \alpha\varepsilon_0, \quad (12)$$

where α is a dimensionless coefficient, which is usually much smaller than 1. Since the length and energy have been defined in units of d_0 and ε_0, there is $E = \alpha/e$.

Thus resistivity is

$$\rho = \frac{E}{J} = \frac{\alpha L^2}{e^2\sum_{x=0}\left[\gamma_{ij}n_i(1-n_j) - \gamma_{ji}n_j(1-n_i)\right]}. \quad (13)$$

In a case when during the hopping event the energy of the initial state is lower than the energy of the final state, the formula of phonon-assisted transition rate γ_{ij} is known

$$\gamma_{ij} = \frac{c_0xy^2}{\beta\varepsilon^3(e^x-1)}. \quad (14)$$

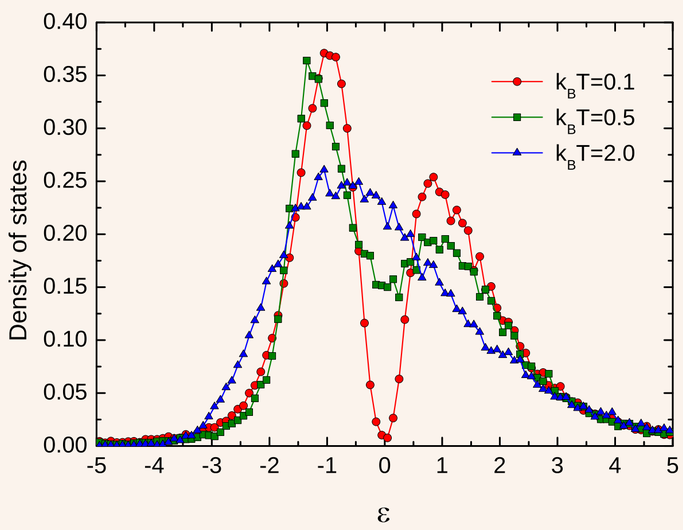

Figure 1: Distribution of the density of energy states at compensation of $b = 0.5$ calculated for three temperatures. Energy and temperature are measured in units of $e^2/\kappa d_0$. Density of states is shown in units of $N_d\kappa d_0/e^2$. Zero of the ε axis coincides with the Fermi energy at each temperature.

Here $x = \beta\Delta\varepsilon_{ij}$, $y = 2r_{ij}/a$, a is localization radius and c_0 is material dependent constant parameter. Since the value of c_0 is arbitrary in this work, it is suitable to set $c_0e^2 = 1$.

The backward transition from site j to i, for which $\Delta\varepsilon_{ij} < 0$, is believed to be spontaneous, and the formula for the rate of such transitions is not known. The rate of such transitions is calculated based on detailed balance condition $\gamma_{ij}n_i(1-n_j) = \gamma_{ji}n_j(1-n_i)$ and it was calculated in a similar manner in this work. Using Eq. 6

$$\gamma_{ji} = \gamma_{ij}\exp\left(\beta\left[\varepsilon_j - \varepsilon_i\right]\right). \quad (15)$$

Since the formula for spontaneous transition rate was obtained using statistical expression for n_i, it is based on mean-field approach. Thus all computational methods currently existing (including Monte Carlo) are at least partially based on mean-field approach. In this sense MC method is inconsistent because it does not reproduce the $n(\varepsilon)$ dependence used to calculate the rate of spontaneous jumps, as was discussed in Section 2.

The energy of hopping transitions had to be calculated as $\Delta\varepsilon_{ij} = \varepsilon_j - \varepsilon_i$ in this work. This means that the self-action effect, which is present if the site energies are calculated using Eq. (5), was disregarded in this work. The reasons and the possible meaning of such an approach are given in the Discussion section.

Since cyclic boundary conditions were assumed, an external electric eddy field is applied to the cell in the direction of the x-axis. The external field modifies the barriers between sites. The hopping energies between sites i and j become

$$\Delta\varepsilon_{ij} = \varepsilon_j - \varepsilon_i + \alpha\Delta x_{ij}, \quad (16)$$

where

$$\begin{aligned}\Delta x_{ij} &= x_j - x_i, \quad |x_j - x_i| \le L/2,\\ \Delta x_{ij} &= -\mathrm{sign}(x_j - x_i)(L - |x_j - x_i|), \quad |x_j - x_i| > L/2,\end{aligned} \quad (17)$$

which is a sign-aware version of Eq. 9.

Thus under applied electric field γ_{ij} will change and a net current will appear in the cell.

Besides changing ε_{ij} and γ_{ij} the electric field will also cause the redistribution of the occupation n_i among the sites. Calculation of these non-equilibrium values of n_i, modified under electric field, is addressed in the next section.

4. Solution of the system of balance equations

In a steady-state, the amounts of charge flowing in and out of site i are equal, which can be written in the form of the charge balance equation

$$\sum_{j\neq i}[\gamma_{ij}n_i(1-n_j) - \gamma_{ji}n_j(1-n_i)] = 0. \quad (18)$$

System of Eqs. 18, written for each site, can be solved with respect to n_i. These equations are, in essence, similar to Kirchhoff's current law and thus represent a non-linearized version of the Miller-Abrahams resistor network method. An important difference, however, is that in Miller-Abrahams method the resistance R_{ij} of each pair is calculated assuming the equilibrium values of n_i. In Eqs. 18, the occupations n_i will change with the applied electric field. Thus field-induced Hubbard current correlations can be partially accounted for using this mean-field approach.

System of Eqs. 18 was used earlier to model carrier mobility in organic semiconductors. The difference of the present approach is that Coulomb interactions and existence of Coulomb gap are taken into account when calculating the energies of the localized states.

The iteration scheme used in this work is the same as one in [Cottaar-2006]. As the initial guess, the equilibrium values of n_i, calculated according to Section 2 were used. System of equations 18 has multiple solutions (for example, $n_i = 0$ is an obvious solution). Thus an additional condition has to be provided to limit the number of solutions to just one. On the other hand, the charge is not conserved during the iteration procedure, and thus, charge conservation ought to be used as a constraint.

Charge conservation was used in this work as an additional condition. To enforce this condition, after each iteration cycle, the change of occupation δn_i was calculated for each impurity site. Sites were divided into two categories with $\delta n_i > 0$ and $\delta n_i < 0$ and sums $\sum|\delta n_i|$ were calculated for each category. Finally, occupation of sites from the category with a larger sum was scaled down in such way that after scaling, the sums of positive and negative δn_i were equal. This procedure guarantees charge conservation and keeps n_i between 0 and 1.

The iterations were carried out in the same random order in which the impurity sites were created. Convergence was always achieved in a wide range of temperatures and electric field intensities.

5. Calculation procedure

Here the summary of the entire calculation procedure is presented. In the first step, a random cell with a given number of primary and compensating defects is generated. Then follows the thermalization procedure in which, according to Section 2, the equilibrium energies and occupation of each site are calculated for a given temperature.

In the next step, two transition rates (γ_{ij} and γ_{ji}) are calculated for each pair of sites using formula Eq. 14 if $\Delta\varepsilon_{ij} \ge 0$ and Eq. 15 if $\Delta\varepsilon_{ij} < 0$. The value of $\Delta\varepsilon_{ij}$ is calculated using Eq. 16. At this step the equilibrium values of ε_i are used.

After this follows the relaxation step in which n_i values are allowed to change under the action of external electric field. The steady-state non-equilibrium values of n_i are found by solution of balance equations, as described in Section 4.

Finally, the resistivity is calculated using Eq. 13.

The presented algorithm does not consider how changes of n_i in the electric field influence the site energies after relaxation and uses equilibrium values of ε_i. It remains to be verified how good such approximation is.

The described procedure was implemented using C++ language and the source code is available at https://gitlab.com/aavdonin/setols.

6. Results

6.1. Temperature dependence

The analysis of temperature dependence of resistivity calculated in the k_BT range between 2.5 and 0.02 is presented in Fig. 2. The calculations were carried out for several cells with different number of impurity atoms (200, 500 and 1000 atoms) to check the influence of the size effect. The compensation coefficient was set to $b = 0.5$; the localization radius a was set to 1/3. The electric field intensity was set to $\alpha = 0.0001$, which means that contribution of the external field to energy is much smaller than both ε_0 and k_BT.

Calculations for 95 data points took respectively 1 min, 62 min and 2 h 58 min for cells with 200, 500, and 1000 impurity atoms on a desktop computer (i5-2400 quad core CPU, 3.1 GHz). The duration depends on the precision settings. The largest change of site occupation after each iteration was used as the convergence parameter $\delta = \max(|n_i^k - n_i^{k-1}|)$, where k is iteration number. In these calculations, the convergence criterion was set to $\delta < 10^{-10}$. The convergence was achieved for all data-points. To decrease the calculation time, nodes with $n_i < \delta_{oc}$ and $1 - n_i < \delta_{oc}$ were disregarded. Here δ_{oc} is the occupation threshold, which is used to filter the nodes with $n \approx 0$ and $n \approx 1$. Such nodes do not contribute significantly to the conductance, according to Eq. 10. In the calculations, δ_{oc} was set to 10^{-10}.

There is no prominent size effect in the results which is due to cyclic boundary conditions employed. However there is a noticeable influence of random realizations even for relatively large cells of 1000 impurity atoms. The calculation time increases fast with the size of the cell but it is also greatly influenced by the realization of the cell. It seems that it is more efficient to make calculations for many small cells and to use some sort of cells-averaging than to make calculations on a single large cell.

The Arrhenius plots of the resistivity are shown in the inset of Fig. 2. The non-linearity of the $\rho(T)$ curves in the Arrhenius

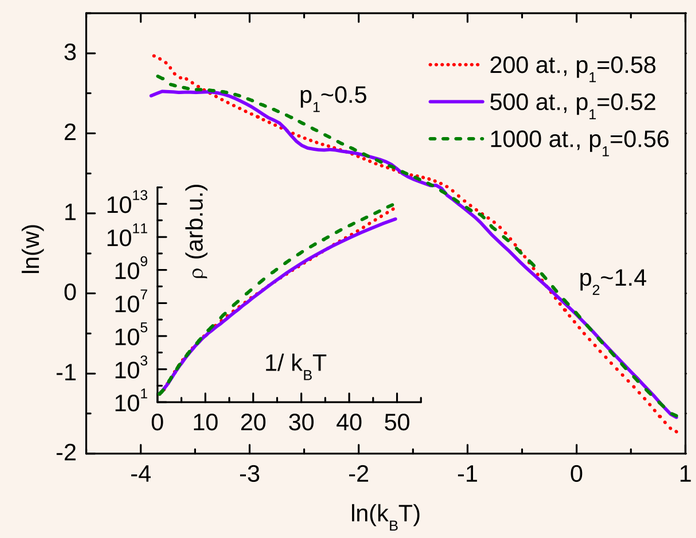

Figure 2: Temperature dependence of the local activation energy w of resistivity calculated for three randomly generated cells with various number of impurity atoms at compensation of $b = 0.5$. Temperature is measured in units of $e^2/\kappa d_0$. Values near the curves show the exponent p of the Mott law. The inset shows the corresponding Arrhenius plots of the resistivity.

plot at low temperatures is a feature specific to hopping transport. In this regime, the resistivity is described by Mott law

$$\rho = \rho_0\exp\left(\frac{T_0}{T}\right)^p, \quad (19)$$

where ρ_0 and T_0 are phenomenological material parameters, and the exponent p is less then one. In a three dimensional sample p is expected to be 0.5. To calculate the value of the exponent p in an objective way, the method of Zabrodskii plot was used in this work. In this method, the argument of the exponential function $w \equiv (T_0/T)^p$ is calculated as

$$w = -\frac{\mathrm{d}\ln\rho}{\mathrm{d}\ln T}, \quad (20)$$

and the result is plotted in a double logarithm scale. In such plot, the slope of a linear region provides the value of p.

These calculations are shown in Fig. 2, where there are two linear regions. Below $k_BT = 0.35$, there is $p \approx 0.5$ for all curves with a precision of about 10%. The behavior of $\rho(T)$ in this region matches well the predictions of the variable range hopping (VRH) theory in the form proposed by Efros and Shklovskii. The linearity in this region is not perfect because the transport depends greatly on the particular distribution of localized sites inside the cell and on the properties of the percolation paths.

Above $k_BT = 0.35$, there is $p \approx 1.4$. I interpret the change of p from 0.5 to 1.4 as the transition from VRH to nearest-neighbor hopping. At nearest-neighbor hopping, a constant hopping energy is expected, which corresponds to $p = 1$. Value of $p = 1.4$ suggests that in this region, the hopping energy is decreasing with the increasing temperature. I attribute this decrease to overlapping of the bands of occupied and empty states and to disappearance of the Coulomb gap, visualized in Fig. 1. This confirms findings from [Avdonin-2019], where a similar decrease of the activation energy at high temperatures was experimentally observed.

There is no crossover from Efros Shklovskii VRH with $p =$

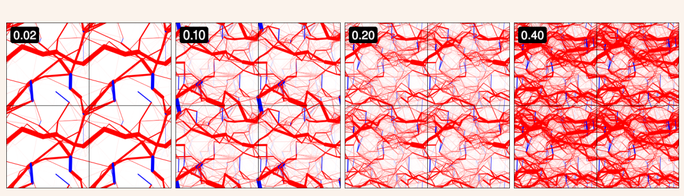

Figure 3: Maps of the electron flow projected on x-y plane, calculated for $k_BT = 0.02$, 0.1, 0.2 and 0.4. Thickness of line segments connecting individual sites is proportional to current between the sites. Localized sites are not shown. Blue color marks segments where current flow is opposite to the applied electric field. Each of the maps shows four adjacent cells produced by shifting the original cell using the CBC.

1/2 to Mott VRH regime with $p = 1/4$ in Fig. 1, which is assumed to happen at partial filling of the Coulomb gap, when DOS at Fermi level becomes non-zero. There is experimental evidence that such crossover occurs, however, there are also reports where such crossover does not occur and references therein). Instead, in this work, there is a direct transition from Efros Shklovskii VRH to nearest-neighbor hopping. A qualitatively similar result was obtained by MC simulations in [Ruiz-1995], however, with $p \approx 1$ in nearest-neighbor hopping regime.

In order to visualize the transition from nearest-neighbor hopping to VRH the evolution of the charge flow with temperature is shown in Fig. 3. The flow maps were calculated for the cell with 500 impurities, which corresponds to the solid purple line in Fig. 2. Maps show the projections of the flow on the x-y plane. The electric field is applied along the x-axis. The thickness of the line segments connecting each pair of impurities i, j is proportional to the current between these defects. To preserve the best contrast, the max value was used for pixel color when parts of the segments have been overlapping. Red color was used for segments when current direction was along the applied field and blue color was used when the current was flowing against the electric field. The flows in all maps are normalized in such a way that the segment with the strongest current in a given map is drawn with the largest width (of 12 pixels) in all maps. The labels on maps show the temperature of the cell.

Above $k_BT = 0.4$ (not shown), there is a very gradual increase in the density of the flow lines and uniformity of the color in the map. Below $k_BT = 0.35$, where the Mott law is observed in Fig. 2, there is a strong reduction of the number of flow paths and appearance of a percolation path at low temperatures.

The blue-colored segments in Fig. 3 correspond to site pairs where current is driven by non-equilibrium concentration gradient rather than by the external field. These segments are usually almost perpendicular to the external electric field direction (x-axis). They appear due to redistribution of the equilibrium occupation during the relaxation procedure.

6.2. Electric field dependence

The current density J in hopping transport shows a non-ohmic dependence on electric field E and in a certain range of field intensities it is often described by $J \sim \exp(\gamma\sqrt{E})$, where γ is a coefficient.

Figure 4 shows the electric field dependence of conductivity calculated using the procedure from this article. Calculations were made for cells of 500 sites at compensation of 0.5. Curves were calculated using the same cell as the one in Fig. 2 at various temperatures, shown near each curve.

It was difficult to make calculations for larger cells because in a limited region of electric fields, the convergence tends to be very slow at $k_BT = 0.02$. It is the region in the vicinity of the bending point where the conductivity mode changes from ohmic to the non-ohmic regime. In the calculation, both the occupation threshold and the convergence criterion were set to 10^{-10}.

Qualitatively our results match the results obtained in [Hayashi-2018]. There is an ohmic region at very small electric fields which is followed by a non-ohmic region in which curves follow the $J \sim \exp(\gamma\sqrt{E})$ law. The ohmic range increases with temperature and γ decreases with temperature (see inset of Fig. 4). On the other hand, there is a much stronger response to electric field, 5 – 6 order of magnitude in this work against 1 – 2 orders of magnitude in [Hayashi-2018]. The source of this difference is not clear. One possible source is in how the density of states is defined in the calculation. In [Hayashi-2018], authors use a constant DOS in a 2D cell. Here the DOS with the Coulomb gap is used in a 3D cell. Another possible source of the difference is in HCC, which are partially accounted for in this algorithm. It was demonstrated in the literature that HCC increase the resistivity by a factor of about two in the ohmic regime. However, the HCC are expected to increase with the electric field, and the influence of HCC can in principle be much stronger. Changes of resistivity as large as 7 orders of magnitude were observed experimentally.

To show that HCC are indeed accounted for (maybe partially) in this method, it is enough to look at the correlation term of the pair current

$$I^C_{ij} = -e(\gamma_{ij} - \gamma_{ji})(< n_in_j > -n^0_in^0_j), \quad (21)$$

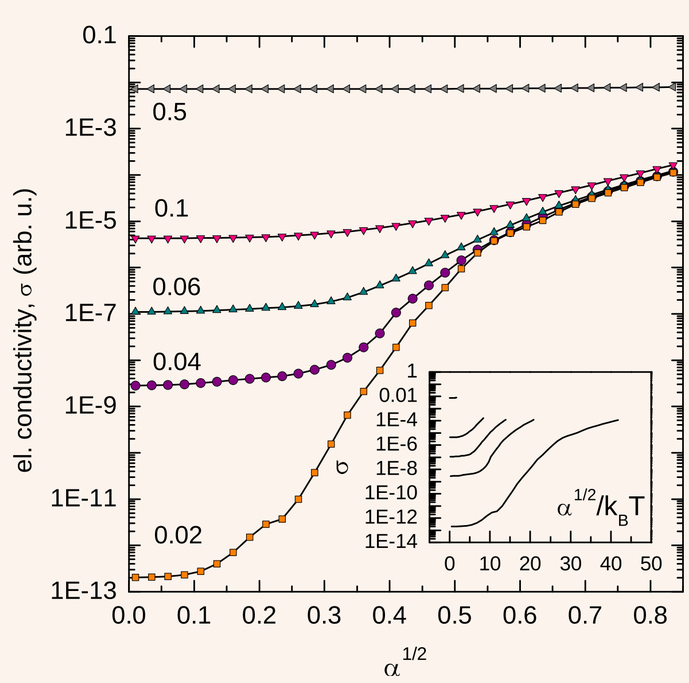

Figure 4: Electrical conductivity in hopping regime vs. square root of the electric field intensity, $\alpha = eEd_0/\varepsilon_0$. Values near each curve show the temperature k_BT of the cell. In the inset: the same data plotted against $\alpha^{0.5}/k_BT$ to show the universal behavior.

where n^0_i is equilibrium occupation of the sites and n_i is occupation under the applied electric field. Due to the relaxation procedure described in Section 4, the correlation current is non-zero in the presented results.

7. Discussion

7.1. Self-action

As was mentioned in Section 3, the self-action correction was not taken into account in this method. To define self-action let us assume that site with index 1 is occupied ($n_1 = 1$) and site 2 is empty ($n_2 = 0$). If site energies are calculated using Eq. (5), then the energy of transition $1 \to 2$ is

$$\varepsilon_{12} = \varepsilon_2 - \varepsilon_1 - 1/r_{12}. \quad (22)$$

Thus $\varepsilon_{12} \neq \varepsilon_2 - \varepsilon_1$ and thus, the last term in Eq. 22 represents the self-action correction. In simple words, the self-action means that the energy of the final state was calculated assuming that the initial state is still occupied.

Such correction is routinely used in MC methods. In the

mean-field approach, however, the correction of self-action is more complicated. This is because both the initial and the final sites always have some finite occupation between 0 and 1. Thus the self-action correction has to be applied to both the initial and the final state. In addition, the transition rate in Eq. (14) is calculated assuming that exactly one electron has been transferred from site i to site j. Thus the transfer energy has to be calculated as if only one electron is present on both sites during the transfer i.e. $n_1 + n_2 = 1$. Such condition is almost never met, and thus, the extra charge $n_1 + n_2 - 1$ has to be removed (or added) from the pair to the surrounding impurities.

The corrected energies of the initial 1 and the final state 2 can be written as

$$\begin{aligned}\varepsilon'_1 &= \varepsilon_1 - \frac{n_2}{r_{12}} + \sum_{k\neq 1,2}\frac{n_1+n_2-1}{r_{1k}},\\ \varepsilon'_2 &= \varepsilon_2 - \frac{n_1}{r_{12}} + \sum_{k\neq 1,2}\frac{n_1+n_2-1}{r_{2k}}.\end{aligned} \quad (23)$$

Here the second term represents the correction of self-action, and the third term represents the correction of the extra charge of the pair transferred to the surrounding sites k. Then the transition energy $\varepsilon_{12} = \varepsilon'_2 - \varepsilon'_1$ is

$$\varepsilon_{12} = \varepsilon_2 - \varepsilon_1 - \frac{n_1-n_2}{r_{12}} + \sum_{k\neq 1,2}(n_1+n_2-1)\left(\frac{1}{r_{2k}} - \frac{1}{r_{1k}}\right). \quad (24)$$

In case when $n_1 = 1$ and $n_2 = 0$ this equation simplifies to usual formula of Eq. 22. When using the Eq. (24), two issues were encountered. First, it is not clear how to distribute the extra charge $n_1 + n_2 - 1$ between the surrounding ions k, since the charge can be distributed in multiple ways. Several approaches were considered. However, non of the approaches helped with the second (and more severe) issue that for some small number of pairs, the sign of the calculated transfer energy ε_{ij} was contradicting the equilibrium occupations n_i and n_j of these sites. It is expected that the energy of transfer from the site with larger occupation to a site with smaller occupation will be positive, i.e. $\varepsilon_{ij} > 0$ if $n_i > n_j$ and vice versa. In the simulation, this condition could not be fulfilled for all pairs.

Unable to fix this controversy, I have postulated that the transfer energy in mean-field approach has to be calculated without self-action. To justify such a decision the following model is proposed. In the mean-field approach the electrons are "smeared" over the available impurity sites with certain probabilities. In such model, one can imagine that only a small fraction of electron charge $\Delta n \ll e$ is transferred at a time from given site 1 to site 2. In such case

$$\varepsilon_{12} = \varepsilon_2 - \varepsilon_1 - \Delta n/r_{12} \approx \varepsilon_2 - \varepsilon_1, \quad (25)$$

and self-action is negligible. In a steady-state small transfers from any given site are compensated by charge-equivalent transfers from the other surrounding sites to the given site. So that no momentary accumulation and depletion of charge occurs on any of sites. The current then occurs as a continuous flow of the smeared electron charge.

This model seems to contradict the entire idea of hopping as a sequence of tunneling events performed by a single electron. However, it might be justified from the perspective of quantum mechanical approach. In such approach each electron will be in a superposition over all impurity states, and even at $T = 0$, none of the sites will have occupation probability of zero or one. The current has to be viewed as the flow of the probability amplitude.

Interestingly, such flow-model takes into account at no extra cost the "multiple electron jump correlations" also called "Coulomb correlations". This is because in the mean-field approach the current flows simultaneously through all pairs. In the MC approach, this kind of correlation is expensive to simulate, even in the case of only two-electron correlations.

8. Summary

Mean-field approach was used to simulate resistivity in hopping regime in a wide range of temperatures and electric fields. The presented method takes into account particularities of the distribution of DOS in the presence of long-range Coulomb interactions. It simulates the Coulomb gap with zero DOS at Fermi level at $T = 0$ and the filling of the Coulomb gap with increasing temperature. It takes into account energy-to-distance correlations of jumps, Hubbard current correlations and multi-electron jump correlations. Most of these features can be simulated only using Monte Carlo simulations.

Compared to the Monte Carlo method, this method is believed to be faster and produces smooth dependencies. It reproduces the Mott law at low temperatures with the power factor of 0.5, in agreement with the prediction of Efros and Shklovskii for the DOS with a Coulomb gap. No transition to Mott variable range hopping regime was observed at higher temperatures. Instead, a direct transition to nearest-neighbor hopping is observed. In this regime, a decrease of activation energy with increasing temperature is predicted. This method also reproduces the ohmic behavior at small electric fields and $J \sim \exp(\gamma\sqrt{E})$ dependence at higher electric fields.

The presented approach has the following inconsistencies. First, the pair transfer rate γ_{ij} was not calculated using mean-field model but using Miller-Abrahams transfer rates based on discrete single-electron tunneling. It is assumed that the mean-field transfer rate is the same. Second, the energies of the sites are not recalculated during the relaxation procedure and are assumed to be close to those at equilibrium. This approximation should be acceptable in the ohmic regime at small electric fields.